



## Deformation of a fluid drop subjected to a uniform electric field

Youness Filali , Mustapha Er-Riani and Mustapha El Jarroudi 

**Abstract.** We theoretically investigate the deformation of a perfect dielectric drop suspended in a second dielectric liquid subject to a uniform electric field. Axisymmetric equilibrium shapes are found by solving simultaneously the Young–Laplace equation at the interface and Laplace equation for the electric field. Analytical solutions are constructed for the governing nonlinear boundary-value problem using domain perturbation method together with a special type of Hermite–Padé approximation. The results show the existence of a critical electric capillary number beyond which no axisymmetric figure is possible.

**Mathematics Subject Classification.** 41A21, 76E25, 35J05.

**Keywords.** Drop deformation, Drop breakup, Electrohydrodynamic effect, Electric capillary number.

### 1. Introduction

Electrohydrodynamic phenomena arise in a broad variety of scientific and engineering applications. These include, among others, inkjet technology [1], electrostatic spraying [2], electrowetting [3], mass spectrometry especially electrospray ionization [4], processes controlled by convection in microgravity [5], and other phenomena in microfluidics [6].

An electric field can also be an effective method for improving heat transfer in nucleate pool boiling process [7].

In meteorology, the shape of the drops in the presence of electric forces has been the subject of many research investigations as diverse as the depolarization of electromagnetic waves in the rain, the study of storms and the investigation of different mechanisms of precipitation formation [8, 9].

In emulsion processes, the application of an electric field makes it possible to characterize the stability of the emulsion and to improve the performance of the surfactants [10].

For the study of the phenomena related to the water/oil interface, the oil after settling is subjected to an electric field which allows the water drops to coalesce and thus create a phase of free water separated from oil [11].

In the following, we briefly review some of the previous works focusing on the influence of an electric field on the behaviour of an isolated fluid drop suspended in another fluid. Special emphasis will be placed on the studies concerning the shapes of this drop and the conditions of their stability. The influence of the various physical parameters of the fluids (permittivities ratio, conductivities ratio, as well as the associated other dimensionless numbers) is conducted.

The deformation of a dielectric drop subject to an electric field has fascinated scientists for generations. The first studies on the effects of electric fields and charges on liquid drops were reported by Franklin in 1751 cf [12].

We mention in this respect the pioneering work of Lord Rayleigh [13] who examined the behaviour of charged drops. He found that an electrically charged drop becomes unstable when the repulsive electrostatic force dominates the attractive surface tension. The drop then breaks up into numerous small drops and leaving behind a stable residual drop. He deduced the criterion of instability for a conductive drop of radius  $a$ , stipulating that the drop remains stable as long as its charge  $q$  is lesser than  $8\pi(a^3\gamma\epsilon_0)^{1/2}$ , where  $\epsilon_0$  is the vacuum permittivity and  $\gamma$  is the surface tension coefficient. This maximum amount of charge that a liquid drop could carry to remain stable, is known as the “Rayleigh limit”.

O’Konski and Thacher [14] studied the deformation of two types of drops: droplets in water clouds and in a dioctyl phthalate oil smoke, immersed in a uniform electric field. They advocate that the droplet elongates in the direction of the field, whether its dielectric constant is higher or lower than that of the surrounding medium, due to the decrease in the total electrostatic free energy of the system which accompanies this distortion in both cases.

In the work of Allan and Mason [15], the deformation and breakup of liquid drops suspended in another immiscible liquid and immersed in a uniform electric field were examined. The authors found that for lower electric field strength values, the deformation of conducting drops into prolate spheroids exhibits a good quantitative agreement with the electrostatic theory. They concluded that breakup behaviour depends on the ratio of the velocity gradient to the electric field strength and the other involved physical parameters.

Garton and Krasucki [16] have shown that a bubble of gas or liquid, under the action of an electric field between two parallel electrodes, takes the form of an elongated spheroid in the direction of the field. They suggested that the bubbles for which the permittivity ratio (denoted  $\kappa$ ) go past the value 20, lengthen until a critical shape is reached, and then the bubbles become unstable. Their experiments have also shown that beyond this critical value, sharp conical tips at the drop poles are formed.

Motivated by the experiments of Allan and Mason, Taylor [17, 18] argued that when the drop and the suspending fluid medium have finite conductivities, surface charges are generated, which in turn lead to circulatory currents inside and outside the drop and bring the interface to an equilibrium state. Additionally, he established a relationship between the ratios of conductivities, viscosities and dielectric constants of the drop and the surrounding medium which allows the drop to remain spherical. Moreover, he gave a criteria describing the circulations that move the surface of the drop towards or away from the poles and to predict whether the drop will become elongated or flattened. Taylor’s model based on this analysis has since come to be known as the leaky dielectric model. A literature review on this model and its applications to phenomena related to electrohydrodynamics was performed by Saville [19].

Rosenkilde [20] used an appropriate extension of the virial method developed by Chandrasekhar, to predict that the drop becomes unstable for sufficiently large electric fields above a threshold of the relative permittivity  $\kappa$  equal to 20.8.

Ajayi [21] extended Taylor’s linearized asymptotic model [18] by including higher-order terms to predict the behaviour of flattened drops; however his study proved insufficient to narrow the gap between theory and experiment. Apparently, this disparity is due to the negligence of nonlinear interfacial charge convection in his model.

By means of the boundary-integral techniques, Miksis [22] had computed the shape of an axisymmetric dielectric drop in a uniform electric field. His results showed that an elongated spheroidal shape is obtained for the permittivity ratio lower than a critical value of the order of 18.08. Beyond this value, the drop will develop for a certain field strength, two obtuse-angled conical tips at its ends known as Taylor cones.

Dodgson and Sozou [23] examined the same problem by considering small perturbations of an elongated spheroid. They obtained a critical permittivity ratio in good accord with that of Rosenkilde.

Sherwood [24] have demonstrated that above the value  $\kappa = 20.8$ , there are three equilibrium figures (two stable and one unstable) for an intermediate range of electric field strengths. Furthermore, he established that the pointed ends are predicted by a numerical scheme when the permittivity of the drop is high relative to that of the surrounding fluid.

Basaran and Scriven [25] used finite-element simulations to argue that at the Rayleigh limit, a family of spherical figures exchange stability with a family of two-lobed shapes through a transcritical bifurcation, of which a branch turns out to be stable.

Li and his co-authors [26] have developed a semi-analytical approach to study the drop deformation in a uniform field, whether electric or magnetic. They showed that beyond a critical value of  $\kappa$  of order 17.59, two conical interfaces with a half opening angle  $\Theta$  are possible, one stable for  $\Theta < 49,3$  and the other unstable for large value of  $\Theta$ . They thus confirmed the result previously obtained by Taylor in [18].

Feng and his co-authors [27] examined numerically the same problem on the basis of the leaky dielectric model. The authors constructed a family of drop shapes exhibiting a turning point when the dimensionless field strength reaches a critical value beyond which no steady solution is possible.

Stone *et al.* [28] developed an analytical expression relating the dependence of the equilibrium cone angle as a function of the ratio  $\kappa$ . When  $\kappa \rightarrow \infty$ , their results compare well with those obtained by Taylor [18] and Li *et al.* [26].

Following the leaky dielectric model formulation, Shaw and his colleagues [29] investigated analytically the drop deformation problem. The results of their analysis suggest that there is a critical value of electric capillary number beyond which no steady states exist and thus bubble disintegration takes place.

In Bjørklund [30] and Paknemat *et al.* [31], the level set method was used to capture the interface of a drop under the application of an electric field in the absence of a net volume charge. Their results enabled them to determine the drop profiles for a wide range of electric capillary numbers  $Ca_E$ , and in particular, to determine the critical value of this number associated with the drop disintegration.

## 2. Electrohydrodynamics equations

First, let's recall that electrohydrodynamics (EHD) is an interdisciplinary research field encompassing several fields including electrostatics and fluid mechanics, where the ohmic model can be a good approximation useful in many cases ([19], [32]).

In this section, we will give an intuitive description of this model and depict the hypothesis behind it. We then propose some physical insights about Maxwell's stress tensor, which plays the crucial role of coupling electrostatic and hydrodynamic effects.

In this work, we will first state the basic electrical laws defining the problem dealt with in this work. An important feature of electrohydrodynamic interactions is that the electric field  $\mathbf{E}$  is irrotational (Electroquasistatic approximation). In addition, dynamic currents are so small that the magnetic induction influence is negligible. Thus the appropriate laws are generally those of electrostatics, as resumed below (see, for example [19], [32]).

$$\nabla \times \mathbf{E} = 0 \quad (1)$$

$$\mathbf{D} = \epsilon \mathbf{E} \quad (2)$$

$$\nabla \cdot \mathbf{D} = q_v \quad (3)$$

$$\mathbf{j} = \sigma_e \mathbf{E} + q_v \mathbf{u} + \frac{\partial \mathbf{D}}{\partial t} \quad (4)$$

$$\nabla \cdot \mathbf{j} + \frac{\partial q_v}{\partial t} = 0 \quad (5)$$

where  $\sigma_e$  is the electrical conductivity,  $\epsilon$  is the dielectric permittivity of the medium and  $\mathbf{u}$  is the fluid velocity field.  $\mathbf{D}$  is the electric displacement vector,  $\mathbf{j}$  the current density and  $q_v$  is the electrical volume charge density.

Equation (3) expresses Gauss's law for electrically linear medium. The current density  $\mathbf{j}$  is the combination of three mechanisms of the current flow: the first term  $\sigma_e \mathbf{E}$  is the Ohmic current which denotes the electrical conduction contribution in the medium, the second term  $q_v \mathbf{u}$  is the convection current and

the last term is due to the variation time of the electric displacement field. Finally Eq. (5) expresses the free charges density conservation.

Although electrical conduction in fluids is often badly characterized by Ohm's law ( $\mathbf{j} = \sigma_e \mathbf{E}$ ), this simple conduction law can be used to draw important conclusions.

For free surface flows in electrohydrodynamics involving a bounded domain  $\Omega$  with regular boundary  $\Gamma$ , as the one treated in this work, we must add to the preceding equations, those resulting from fluid mechanics, namely the continuity equation and the momentum conservation:

$$\frac{\partial \rho}{\partial t} + \nabla \cdot (\rho \mathbf{u}) = 0 \quad (6)$$

$$\frac{\partial(\rho \mathbf{u})}{\partial t} + \rho(\mathbf{u} \cdot \nabla) \mathbf{u} = \nabla \cdot (-p \mathbf{I} + \mu(\nabla \mathbf{u} + \nabla \mathbf{u}^T) + \boldsymbol{\sigma}^M) + \rho g \mathbf{n}_g + \gamma C \delta_\Gamma \mathbf{n} \quad (7)$$

where  $\rho$  is the fluid density,  $p$  the pressure field,  $\mathbf{I}$  the identity tensor,  $\mu$  the dynamic viscosity,  $\gamma$  the surface tension coefficient,  $C$  the mean interface curvature,  $\delta_\Gamma$  the Dirac measure at the interface  $\Gamma$ ,  $g$  is the gravitational acceleration and  $\boldsymbol{\sigma}^M$  the Maxwell stress tensor.  $\mathbf{n}$  and  $\mathbf{n}_g$  denote, respectively, the normal at the interface and the unit gravity vector. Recalling that the Maxwell stress tensor is defined by:

$$\boldsymbol{\sigma}^M = \epsilon(\mathbf{E} \otimes \mathbf{E} - \frac{1}{2} E^2 \mathbf{I}) \quad (8)$$

The electric forces density  $\mathbf{F}_e$  is related to the Maxwell stress tensor by the relation:  $\mathbf{F}_e = \nabla \cdot \boldsymbol{\sigma}^M$ .

In most macroscopic flow studies, the influence of an external electric field on a moving fluid can be neglected, as shown by a simple analysis of the order of the magnitude of the forces involved. The electric force must be taken into account when the scale of the flow is small, since externally applied electric fields (even when relatively small) can have a significant effect on a flow, especially when considering cases of multiphase flows. Moreover, in the dielectric formulation proposed by Taylor (leaky dielectric), the electric force is important only when there is a gradient or a jump in electrical conductivity  $\sigma_e$  and/or in the permittivity  $\epsilon$ . Since this two-phase fluid model is observed at such small scales, the effects of capillary forces must be taken into account in the momentum equation (last term of Eq. 7).

### 3. Governing equations

In this section, we will determine the axisymmetric equilibrium figures of an incompressible perfect dielectric drop, suspended in another incompressible fluid without free charge density. The problem will be set in a reference frame  $(\mathbf{e}_x, \mathbf{e}_y, \mathbf{e}_z)$  with the origin attached to the drop centre. By applying an external electric field  $\mathbf{E}_\infty$ , parallel to the gravity direction, i.e.  $\mathbf{E}_\infty = -E_\infty \mathbf{e}_z$ , the drop becomes deformed. Its shape is determined by the local balance of the surface tension and external forces corresponding here to the gravity and the electric force. Surface tension tends to make the drop spherical, whereas gravity tends to flatten it. Typically, the external electric field tends to lengthen it along its direction.

We will consider the special case of a smooth axisymmetric drop that occupies a domain  $\Omega_1$ , exhibiting symmetry of revolution about the axis  $Oz$  and symmetrical with respect to the plane  $Oxy$ . We denote by  $\partial\Omega_1$  the boundary of  $\Omega_1$  and by  $\mathbf{n}$  its outward unit normal vector. The surrounding fluid occupies the domain  $\Omega_2 = \mathbf{R}^3 - \Omega_1$ . The situation is portrayed in Fig. 1.

The electric field discontinuity across the interface creates a jump of Maxwell's stress tensor denoted by  $\Delta P_e = [\mathbf{n} \cdot \boldsymbol{\sigma}^M \cdot \mathbf{n}^T]$  that is similar to an electric pressure, where the notation  $[(\cdot)]$  represents the jump across the interface of the quantity “ $(\cdot)$ ” inside the brackets.

Given the relation (8), the external and internal Maxwell stress  $\sigma_e^M$ , respectively,  $\sigma_i^M$  at the drop, can be expressed in terms of tangential ( $E_t$ ) and normal ( $E_n$ ) components of the electric field by the relations

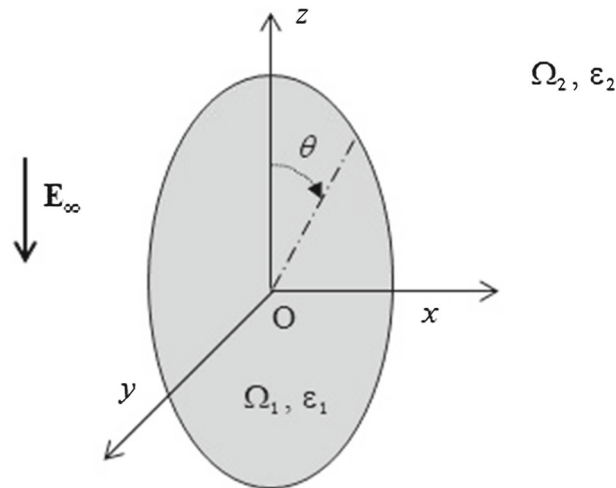


FIG. 1. Schematic diagram of the problem setup

(see for example, Sherwood [24])

$$\sigma_i^M = \frac{1}{2}\epsilon_1(E_{1n}^2 - E_{1t}^2), \quad \sigma_e^M = \frac{1}{2}\epsilon_2(E_{2n}^2 - E_{2t}^2) \quad (9)$$

where  $\epsilon_i$ , ( $i = 1, 2$ ) is the dielectric constant of medium  $i$ .

If the two media are perfect dielectrics with zero electrical conductivity, then the continuity of the electric field tangential components is satisfied, i.e.  $E_{1t} = E_{2t} = E_t$ . Therefore, the jump of the normal electrical stress across the interface separating the two dielectric media can be written as follows:

$$\Delta P_e = \sigma_e^M - \sigma_i^M = \frac{1}{2}(\epsilon_2 E_{2n}^2 - \epsilon_1 E_{1n}^2 + (\epsilon_1 - \epsilon_2) E_t^2) \quad (10)$$

Because there is an interface between two dissimilar dielectric media, the boundary conditions can then be expressed as:

$$\epsilon_1 E_{n1} = \epsilon_2 E_{n2} \quad (11)$$

Then it follows that the electric pressure may be written in the form:

$$\Delta P_e = \frac{1}{2}(\epsilon_1 - \epsilon_2) \left[ \frac{\epsilon_1}{\epsilon_2} E_{n1}^2 + E_t^2 \right]$$

In other words, this relation can be expressed by the general formula:

$$\Delta P_e = \frac{1}{2}\epsilon_2(\kappa - 1) [\kappa E_{n1}^2 + E_t^2] \quad (12)$$

where  $\kappa = \frac{\epsilon_1}{\epsilon_2}$  is the ratio of the two media dielectric constants.

The equilibrium shape of a charged drop can be determined from the condition that local interfacial forces must be in balance at each point on the surface resulting in the so-called augmented Young–Laplace equation [25]:

$$\gamma C = \Delta P_0 + \Delta \rho g z + \Delta P_e \quad (13)$$

where  $\gamma$  is the surface tension coefficient,  $C$  is the interface mean curvature of  $\partial\Omega_1$ ,  $\Delta P_0$  is the difference in pressure across the drop interface,  $\Delta \rho$  is the density difference between the drop and surrounding fluid,  $g$  is the acceleration due to gravity, and  $z$  is the vertical distance measured from the origin in the opposite direction to gravity.

When the drop is a perfect dielectric liquid with no free charge density at the interface, then the electric tangential stress will be zero. Thus, the equation governing the equilibrium shape, i.e. Eq. (13), is reduced to:

$$\gamma C = \Delta P_0 + \Delta \rho g z + \frac{1}{2} \epsilon_1 (\kappa - 1) E_{n1}^2 \quad (14)$$

We will assume that the drop is static under the electric field and that the effects of gravitational forces are negligible compared to the effects of electrostatic forces. In the absence of fluid movement, Eq. (14) reflects the fact that the drop shape results from the equilibrium between surface tension and electrical pressure at the interface.

In the absence of the electric field, the equilibrium shape is a spherical domain  $\Omega_0$  of radius  $R$ . A spherical coordinate system  $(r, \theta, \psi)$  has to be assumed, with the origin at the centre of the drop and with the  $z$  direction as the symmetry axis.  $\psi$  is the azimuthal direction angle and  $\theta$  is the angle of the meridian measured from the axis of symmetry as shown in Fig. 1.

The electric field  $\mathbf{E}$  can be expressed as :  $\mathbf{E}_1 = \nabla u_1$  and  $\mathbf{E}_2 = \nabla u_2 + \mathbf{E}_\infty$ , where  $u_1$  and  $u_2$  are the electrostatic potentials outside and inside the drop, with  $u_2 \rightarrow 0$  and  $\nabla u_2 \rightarrow 0$ , as  $r \rightarrow \infty$ .

By introducing the following dimensionless variables :  $\bar{C} = RC$ ,  $\mathbf{E} = E_\infty \bar{\mathbf{E}}$ ,  $\mathbf{x} = R\bar{\mathbf{x}}$ ,  $u = E_\infty R\bar{u}$ , the equations governing the electrostatic problem become:

$$\Delta \bar{u}_i = 0 \quad \text{in } \Omega_i \quad i = 1, 2. \quad (15)$$

$$\frac{\lambda}{2} (\kappa - 1) [\kappa \bar{E}_{n1}^2 + \bar{E}_{t1}^2] - \bar{C} + K = 0 \quad \text{on } \partial\Omega_1 \quad (16)$$

where

$$\lambda = \frac{\epsilon_2 R E_\infty^2}{\gamma} = Ca_E, \quad K = \frac{R \Delta P_0}{\gamma} \quad (17)$$

with  $E_\infty$  is the electric field magnitude far from the drop,  $Ca_E$  is the electric capillary number which is the ratio of electrical stress to surface tension. The dimensionless parameter  $K$  is related to the difference between the drop and the ambient pressure. This unknown constant can be determined by constraining the drop volume to be fixed at  $V_0$ :

$$V = V_0 = \frac{4\pi}{3} R^3 \quad (18)$$

For axisymmetrical shapes, the radial shape function is described in spherical coordinates as  $r = Rf(\theta, \lambda)$  where  $f(\theta, \lambda)$  is the dimensionless shape function of the drop. From now, the bars will be dropped for clarity.

The governing equations (15, 16) are subject to the following boundary conditions:

$$f_\theta = 0, \quad \text{at } \theta = 0, \pi, \quad (19)$$

$$u_1 = u_2 - \cos \theta \quad \text{and} \quad \frac{\partial u_2}{\partial n} - \mathbf{e}_z \cdot \mathbf{n} - \kappa \frac{\partial u_1}{\partial n} = 0 \quad \text{on } \partial\Omega_1 \quad (20)$$

where  $f_\theta = \frac{df}{d\theta}$ , and the symbol  $\frac{\partial}{\partial n}$  denotes differentiation with respect to the outward normal derivative on  $\partial\Omega_1$ .

According to Gauss's law, the Laplace equation (15) governs the electrostatic potential behaviour inside and outside the drop. The normal stress balance (16) deduced from the Bernoulli equation for the static drop is a modified form of the Laplace–Young equation that includes the contribution of the electrostatic pressure. The condition (19) is necessary for the drop to be axisymmetric, while relations (20) represent, respectively, the electrostatic potential continuity and the electric displacement at the interface, separating the two dielectric media.

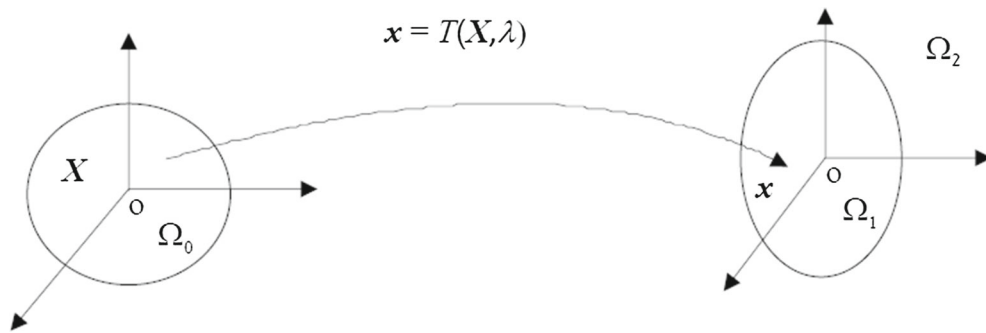


FIG. 2. Lagrangian representation

#### 4. Method of solution

In this section, we will use the domain perturbation method developed by Joseph [33] that allows us to construct an analytical solution to the problem (15-20). The idea behind this approach is to consider as principal unknown the transformation field  $\mathbf{x} = T(\mathbf{X}, \lambda)$  from the initial known domain  $\Omega_0$ , taken as a reference position, to the unknown position  $\Omega_1$  (see Fig. 2). Therefore, the actual calculation will be carried out on the unperturbed domain. Thereby this perturbation analysis approach is used to study of the effect of a small electrical field on the stability of a nearly spherical drop.

Let  $T$  be a domain transformation of class  $C^2$  that maps the spherical domain  $\Omega_0$  to the unknown domain  $\Omega_1$ :

$$\begin{cases} T : \Omega_0 \rightarrow \Omega_1 \\ \mathbf{X} \mapsto \mathbf{x} = T(\mathbf{X}, \lambda) \end{cases}$$

The transformation field form can be written as:  $T = rf(\theta, \lambda)\mathbf{e}_r$ , where  $\mathbf{e}_r, \mathbf{e}_\theta, \mathbf{e}_\psi$  are the usual unit vectors in spherical coordinates.

Now under these considerations, the potential  $u$  can be written as :  $u(x, y, z) = v(r, \theta, \lambda)$ .

The equations transported back to the reference configuration  $\Omega_0$  are given by:

$$\begin{cases} \nabla \cdot (|\det T'| T'^{-1} {}^t T'^{-1} \nabla v_1) = 0 & \text{for } r < 1 \\ \nabla \cdot (|\det T'| T'^{-1} {}^t T'^{-1} \nabla v_2) = 0 & \text{for } r > 1 \\ v_1 = v_2 - \cos \theta & \text{for } r = 1 \\ {}^t T'^{-1} \nabla v_2 \cdot {}^t T'^{-1} \mathbf{e}_r - {}^t T'^{-1} \mathbf{e}_z \cdot {}^t T'^{-1} \mathbf{e}_r - \kappa {}^t T'^{-1} \nabla v_1 \cdot {}^t T'^{-1} \mathbf{e}_r = 0 & \text{for } r = 1 \\ v_2 \rightarrow 0 \text{ and } \nabla v_2 \rightarrow 0, \text{ as } r \rightarrow \infty & \end{cases} \quad (21)$$

Where  $T', T'^{-1}, {}^t T'$  denote, respectively, the Jacobian, the inverse and the transpose of the Jacobian. Equation (16) is transformed into a relation expressing the scalar potential  $v$  and the shape function  $f$  as follows:

$$\lambda \frac{(\kappa - 1)}{2} \left[ \kappa \left( {}^t T'^{-1} \frac{\partial v_1}{\partial r} \right)^2 + \left( \frac{1}{r} {}^t T'^{-1} \frac{\partial v_1}{\partial \theta} \right)^2 \right] - C + K = 0 \quad (22)$$

The mean curvature is written in terms of the shape function as:

$$C = -\frac{f f_{\theta\theta} - f_\theta^2 - f^2}{(f^2 + f_\theta^2)^{3/2}} - \frac{f_\theta \cos \theta - f \sin \theta}{f \sin \theta (f^2 + f_\theta^2)^{1/2}} \quad (23)$$

The reference pressure  $K$  depending only on  $\lambda$  is calculated by requiring the drop volume to be fixed by the constraint (18) i.e.:

$$\int_0^{\pi/2} f^3 \sin \theta d\theta = 1 \tag{24}$$

Therefore, the first equations of the system (21) can be written in the form:

$$[F_{1i}]_r + \frac{2}{r} [F_{1i}] + \frac{1}{r} [F_{2i}]_\theta + \frac{\cos \theta}{r \sin \theta} [F_{2i}] = 0 \quad i = 1, 2 \tag{25}$$

with  $F_{1i} = \left[ (f^2 + f_\theta^2) v_{ir} - \frac{f_\theta v_{i\theta}}{r} \right]$ ,  $F_{2i} = \left( \frac{f}{r} v_{i\theta} - f_\theta v_{ir} \right)$ ,  $i = 1, 2$ . The boundary conditions are reduced for  $r = 1$ , to the following relations :

$$\begin{cases} v_1 = v_2 - \cos \theta \\ (f^2 + f_\theta^2)(v_{2r} - \kappa v_{1r}) - f f_\theta (v_{2\theta} - \kappa v_{1\theta}) = (f^2 + f_\theta^2) \cos \theta + f f_\theta \sin \theta \end{cases} \tag{26}$$

and the modified Young–Laplace equation becomes:

$$\lambda \frac{\kappa - 1}{2} \left[ \kappa v_{1r}^2 \left( 1 + \frac{f_\theta}{f} \right)^2 + v_{1\theta}^2 \right] + (K - C) f^2 = 0 \tag{27}$$

The advantage of this procedure is that the equations and boundary conditions can be rewritten with respect to a fixed reference domain, and in addition explicit equations estimating the shape function  $f$  are obtained. The major drawback is that these equations are a little more arduous. Noticing that for  $\lambda = 0$ , there is a solution:  $f(\theta, 0) = 1$ , and  $v(r, \theta, 0)$ . Using the implicit function theorem [34], we can assert the existence of a unique solution depending only on  $r, \theta$  and analytic in  $\lambda$ . Therefore, the above functions  $v, K$  and  $f$  can be expressed as a power series expansion in  $\lambda$ , for sufficiently small  $\lambda$ :

$$\begin{cases} v_1 = v_1(r, \theta, \lambda) = \sum_{n \geq 0} \lambda^n s_n(r, \theta), \quad \text{for } r < 1 \\ v_2 = v_2(r, \theta, \lambda) = \sum_{n \geq 0} \lambda^n t_n(r, \theta), \quad \text{for } r > 1 \\ f = f(\theta, \lambda) = \sum_{n \geq 0} \lambda^n g_n(\theta) \\ K = \sum_{n \geq 0} \lambda^n h_n \end{cases} \tag{28}$$

We first insert the relations (28) into the governing Eqs.(25-27) and collect the coefficients of similar powers of  $\lambda$ , to obtain a sequence of perturbation problems containing differential equations with their associated boundary conditions. We note that the system of equations is uncoupled at each order, in the sense that the equations of the potential at order  $m + 1$  depend only on solutions of lower-order problems. At each order, we firstly integrate the equation derived from (25) with respect to  $s_n(r, \theta)$  and  $t_n(r, \theta)$  subjected to the boundary conditions (26). Secondly, we insert these values into (27) to get the expression for  $g_n$ , which enclose an unknown constant of the reference pressure  $h_n$ . This constant has to be calculated by taking into account Eq. (24). In addition, these equations turn out to have solutions as linear combination of Legendre’s polynomials. We can thus write:

$$s_n(r, \theta) = \sum_{m \geq 0} a_n^m(r) P_m(\xi), \quad t_n(r, \theta) = \sum_{m \geq 0} b_n^m(r) P_m(\xi), \quad g_n(\theta) = \sum_{m \geq 0} c_n^m P_{2m}(\xi) \tag{29}$$

with  $\xi = \cos \theta$ . Furthermore, we derive equations for  $a_n^m(r)$ ,  $b_n^m(r)$  and  $c_n^m$  which are submitted to condition (24), enabling us to calculate  $h_n$ .



In what follows, we will examine the first few orders:

**Order 0:**

The Laplace–Young equation gives:  $h_0 = 2$ . The equations for potential are:

$$\begin{cases} \Delta s_0 = 0 & \text{for } r < 1 \\ \Delta t_0 = 0 & \text{for } r > 1 \\ t_0 - s_0 = -1 & \text{for } r = 1 \\ \frac{\partial t_0}{\partial r} - \kappa \frac{\partial s_0}{\partial r} = 1 & \text{for } r = 1 \\ t_0 = -\cos \theta & \text{as } r \rightarrow \infty \end{cases}$$

whose solutions are:

$$s_0(r, \theta) = -3\alpha r \xi, \quad t_0(r, \theta) = -\xi + \frac{\alpha(\kappa - 1)\xi}{r^2}, \quad \text{where } \alpha = \frac{1}{\kappa + 2}.$$

**Order 1:** The Laplace–Young equation is reduced to:

$$\frac{d^2 g_1}{d\theta^2} + \frac{\cos \theta}{\sin \theta} \frac{dg_1}{d\theta} + 2g_1 = \frac{1}{2}(\kappa - 1) \left[ \kappa \left( \cos \theta \frac{\partial s_0}{\partial r}(1, \theta) \right)^2 + \left( \sin \theta \frac{s_0(1, \theta)}{r} \right)^2 \right] + h_1$$

Taking into account (29) and injecting the expressions of  $s_0(r, \theta)$  into the relation above yields:

$$g_1(\theta) = \beta_1(3P_2(\xi) - 1), \quad \text{where } \beta_1 = \frac{3}{8}(\kappa - 1)^2 \alpha^2.$$

The constraint on the volume gives:

$$h_1 = -\frac{1}{2} \alpha^2 \kappa (\kappa - 1) \sigma_1, \quad \text{where } \sigma_1 = 5\kappa^2 + 8\kappa + 14.$$

The analysis can in principle be carried out to obtain terms of higher order, but the task becomes tedious and cumbersome. Using a computer algebra system, we obtained the first 15 terms of the solution series (28). Thus in spherical coordinates, the radial position of the interface is given up to order 2 by:

$$f(\theta, \lambda) = 1 + \beta_1 [3P_2(\xi) - 1] \lambda + \beta_2 [5(\kappa + 2)(21\kappa^2 + 55\kappa - 20)P_4(\xi) + 6(-39\kappa^3 + 74\kappa^2 + 292\kappa - 192)P_2(\xi) + 69\kappa^3 - 217\kappa^2 - 682\kappa - 376] \lambda^2 + O(\lambda^3) \quad (30)$$

$$\text{with } \beta_2 = -\frac{3}{40} \frac{\alpha \beta_1 (\kappa - 1)}{(3\kappa + 4)}.$$

## 5. Bifurcation study

### 5.1. Objective and general principles

The equilibrium states of a perfect dielectric drop in a uniform electrostatic field in dimensionless form, i.e. Eqs.(15-20), are determined as solutions of a functional equation of the form  $G(\lambda, \phi) = 0$ , where  $\phi = (v, f, K)$  is an element of a Banach space  $\mathcal{E}$ , and  $G$  is a mapping from  $\Lambda \times \mathcal{E}$  to another Banach space  $\mathcal{F}$ ,  $\Lambda \subset \mathbf{R}$ . The implicit function theorem [34] ensures the existence and uniqueness of a solution provided that the linear operator  $L(\lambda) = \frac{\partial G}{\partial \phi}(\lambda, \phi)$  is invertible in a neighbourhood of  $\lambda = 0$ . In general, the operator  $L(\lambda)$  has a discrete spectrum. If none of its eigenvalues vanish, the operator is then invertible and therefore, there exists a unique solution to  $G(\lambda, \phi) = 0$ . Suppose that as  $\lambda$  crosses a critical value  $\lambda_c$ , one or more eigenvalues of  $L(\lambda)$  becomes zero, then the operator  $L(\lambda)$  is no longer invertible, which is a condition for  $\lambda_c$  to be a bifurcation point or a limit point. For further details, see the reference [34].

For perturbation problems, a specific method for calculating bifurcation points can be performed by analysing the obtained solution series. In this case, bifurcation points are related to the values of convergence radius of these solutions (point where analyticity fails). However, the difficulty lies in determining these parameters directly from the classical ratio test. In fact, most perturbation series have a finite

number of terms as the case examined here. So it's difficult to estimate more precisely the radius of convergence. Moreover, these calculations cannot be done without the aid of a computer algebra system. Besides, this approach suffers from what is called intermediate expression swell or combinatorial explosion causing the RAM exhaustion.

The aim of analysis series is to obtain from the first  $N$  coefficients, as accurately as possible, the convergence radius namely the distance to the origin of the nearest singularity. We should report that there exists several methods devised for extracting estimates of the critical parameters from a finite number of series coefficients. The most commonly used methods are the ratio method, initially developed by Domb and Sykes and expanded by many authors, and semi-numerical approximant methods, such as Padé approximants [35], Hermite–Padé approximants [36], etc. For our part, we use a new form of differential approximants (see references [37], [38]) which are a subclass of Hermite–Padé approximants. This method has proved to be a useful tool in many branches of physics and applied mathematics to determine the singularities of a function from its power series expansion, as well as estimate it on its branch cuts. It consists of a high-order linear differential equation with polynomial coefficients that is satisfied approximately by the partial sum of a power series.

## 5.2. The basic procedure

In the previous section, we have examined the analytic structure of the solution series (28). Once this is realized, the next step is to locate the nearest singularity limiting the convergence of these series and to examine its nature. This singularity should be real and positive in order to have a physical sense. Suppose that  $U(\lambda)$  is an analytic representation of an unknown function  $u(\lambda)$ , i.e.

$$U(\lambda) = \sum_{n=0}^{\infty} d_n \lambda^n \text{ as } \lambda \rightarrow 0 \quad (31)$$

It has been reported above that only a limited number of coefficients (say  $N$ ) can be determined. We are interested to study the bifurcation by analytic continuation as well as the dominant behaviour of the solution by using the partial sum :

$$U_N(\lambda) = \sum_{n=0}^{N-1} d_n \lambda^n \quad (32)$$

It is well known that the singularity must be either an algebraic pole or a logarithmic branch point (cf. [35]). So  $U(\lambda)$  takes the form:

$$U(\lambda) \sim \begin{cases} A(\lambda_c - \lambda)^\gamma \text{ for } \gamma \neq 0, 1, 2, \dots, \\ A(\lambda_c - \lambda)^\gamma \ln|\lambda_c - \lambda| \text{ for } \gamma = 0, 1, 2, \dots, \end{cases} \text{ as } \lambda \rightarrow \lambda_c \quad (33)$$

where  $A$  is some constant and  $\lambda_c$  is the critical point with the critical exponent  $\gamma$ .

In order to extract this singularity, we will adopt the same approach as in ([37], [38]) based on differential Hermite–Padé approximants.

Let us recall that these approximants are obtained by identifying polynomials  $A_{mN}$  such that:

$$A_{0N}(\lambda) + \sum_{m=1}^M A_{mN}(\lambda) U^{(m)}(\lambda) = O(\lambda^m) \text{ as } \lambda \rightarrow 0 \quad (34)$$

with  $\sum_{m=0}^M \deg A_{mN}(\lambda) + M = N$ , and  $U^{(m)}(\lambda) = D^{m-1}U(\lambda)$ , where  $D$  is the differential operator given by  $D = \frac{d}{d\lambda}$ . In addition, we normalize the polynomials (34) by setting  $A_{0N}(\lambda) = 1$ , in order to obtain as many equations as unknowns. In practice, we often take  $M = 3$ , we believe that this choice will lead us to detecting physical singularities as Common did in his work [36].

TABLE 1. Calculations showing the rapid convergence of the procedure corresponding to the bifurcation point for the aspect ratio  $e(\lambda)$  for different values of  $\kappa$

$M$	$N$	$\kappa = 50$	$\kappa = 30$	$\kappa = 20$	$\kappa = 10$
		$\lambda_{cN}$	$\lambda_{cN}$	$\lambda_{cN}$	$\lambda_{cN}$
1	9	0.1952336959	0.2125246851	0.2354803662	0.3141845313
2	12	0.1948455186	0.2120644074	0.2349496492	0.3134597348
3	15	0.1946919163	0.2118288164	0.2346965164	0.3128976634

The dominant singularities associated to (34) turn up to be the zeros of the leading polynomial  $A_{3N}(\lambda)$ . The nearest singularity  $\lambda_c$  is the smallest one, and the critical exponent  $\gamma_N$  may be estimated by

$$\gamma_N = 1 - \frac{A_N^{(M-1)}(\lambda_{c,N})}{DA_N^{(M)}(\lambda_{c,N})} \quad (35)$$

## 6. Results and discussion

The equilibrium shapes and stability of perfect dielectric drop in an external electric field, are governed by two parameters: the electrical permittivity ratio  $\kappa$  and the electric capillary number  $CaE = \lambda$  which measures the relative importance of electrical stress and surface tension in setting drop shape.

The Hermite–Padé approximation procedure in Sect. 5 was applied to the first 15 terms of the solution series obtained in Sect. 4. This procedure makes it possible to evaluate that for every value of  $\kappa$ , there is a critical value  $\lambda_c$  (a limit or bifurcation point) such that, for  $0 < \lambda < \lambda_c$ , the axisymmetric drop shapes are stable but at  $\lambda_c$  lose stability to give rise to a unstable equilibrium shapes family. By means of energy arguments O’Konski and Thacher [14], Garton and Krasucki [16], and Sherwood [24], have shown that only prolate equilibrium shapes are those that minimize the total energy defined as the sum of the surface energy and the electric energy. This energy minimization procedure shows that the prolate shape family remains stable for  $\lambda < \lambda_c$ , which is a typical case of a subcritical bifurcation.

In the following, we first illustrate how the obtained series solutions will permit us to identify the nature and location of the nearest singularity to the origin. Secondly, we show that this singularity corresponds to a bifurcation point. To do this, we employ the differential approximants of Hermite–Padé, and the results are reported in Tables 1, 2 and 3. This approach will first be applied to analyse the aspect ratio  $e(\lambda) = \frac{R_p}{R_e}$ , where  $R_e$  and  $R_p$  denote, respectively, the equatorial and polar radius of the drop. The series corresponding to  $e(\lambda)$  can be written as

$$e(\lambda) = \sum_{n \geq 0} p_n \lambda^n \quad (36)$$

Table 1 shows the rapid convergence of the dominant singularity  $\lambda_c$  for different values of the ratio of the dielectric permittivities  $\kappa$ , with a gradual increase in the coefficients number of the series (36) used in the approximants.

By similar calculations, we proceeded to extract the nearest singularities to the origin corresponding to the semi-axis  $R_e$ ,  $R_p$  and to the reference pressure  $K$  (cf. Table 2). We found values roughly equal to that of the aspect ratio.

Results for higher permittivity ratios are included in Table 3. We notice from Tables (1-3) that the estimates of  $\lambda_c$  decrease as  $\kappa$  increases.

In the following, we will proceed to a comparison between the results obtained by this analytical approach and those existing in the literature. We have contented ourselves with a comparison with results from authors who neglected the conductivities of the two media, as is the case dealt with in this

TABLE 2. Calculations showing the rapid convergence of the procedure corresponding to the bifurcation point for the reference pressure  $K(\lambda)$  for different values of  $\kappa$

$M$	$N$	$\kappa = 50$ $\lambda_{cN}$	$\kappa = 30$ $\lambda_{cN}$	$\kappa = 20$ $\lambda_{cN}$	$\kappa = 10$ $\lambda_{cN}$
1	9	0.1948402612	0.2119338761	0.2346419210	0.3140346307
2	12	0.1947895390	0.2119627307	0.2348031756	0.3134296352
3	15	0.1946632718	0.2118613095	0.2347029490	0.3129595439

TABLE 3. Critical electric capillary number vs  $\kappa$

Value of $\kappa$	28	30	50	100
Critical values of $Ca_E$	0.2154186097	0.2118288164	0.1946919163	0.1827286575

TABLE 4. Comparison of critical values of the electric capillary number versus the permittivity ratios  $\kappa$

Value of $\kappa$	Taylor [17]	Sherwood [24]	Dodgson and Sozou [23]	Present work
$\epsilon_1 \rightarrow \infty$	0.20976	0.20430	0.20453	0.1717632540
28.2			0.21	0.2146655392
25		0.31		0.2208122145
20		0.36	0.34784	0.2346998806
1		0.24		0.2478126749

work. The results are listed in Table 4. We note that for certain values of  $\kappa$ , in particular when  $\epsilon_1$  is very large, the values obtained are significantly different. However for some cases, the values obtained are slightly different.

Depending on the value of the parameter  $\kappa$  and the strength field i.e.  $\lambda$ , the drop deforms into a flattened or elongated spheroid as shown in Figs. 3, 4, 5, 6, 7, 8 and 9, but as we mentioned before, only the elongated shapes are stable for  $\lambda < \lambda_c$ , unstable otherwise because the drop depart from its local energy minimum; these drops are rarely observed in experiments. This joins the result of Taylor [18] who deduced on theoretical bases that an uncharged drop becomes unstable at a turning point in the applied field strength.

This behaviour can also be examined by considering the Taylor deformation parameter defined by  $D_{Taylor} = (R_p - R_e)/(R_e + R_p)$ . Positive and negative values of  $D_{Taylor}$  stand for prolate and oblate shapes, respectively. Using the relation giving the dimensionless shape function of the drop, as stated in Eq. (28), we obtain:

$$D_{Taylor} = C_1(\kappa)\lambda + C_2(\kappa)\lambda^2 + O(\lambda^3) \tag{37}$$

with

$$C_1(\kappa) = \frac{3\beta_1}{2}, C_2(\kappa) = \frac{9}{16}\beta_1^2 - \frac{\beta_2}{16}(2283\kappa^3 - 7753\kappa^2 - 23274\kappa + 14824)$$

We observe that at order 1, this formula coincides with that established by Allan and Mason [15] and O’Konoski and Thacher [14]. The evolution of this parameter is shown in Fig. 3 for different values of the permittivity ratio. This figure illustrates that for  $\kappa$  less than a critical value  $\kappa_c = 18$ , the drop profile is flattened at higher field strengths, although for values greater than  $\kappa_c$ , the figure is lengthened, which is valid regardless of the value of the electric field strength. This is clearly shown by plotting the aspect

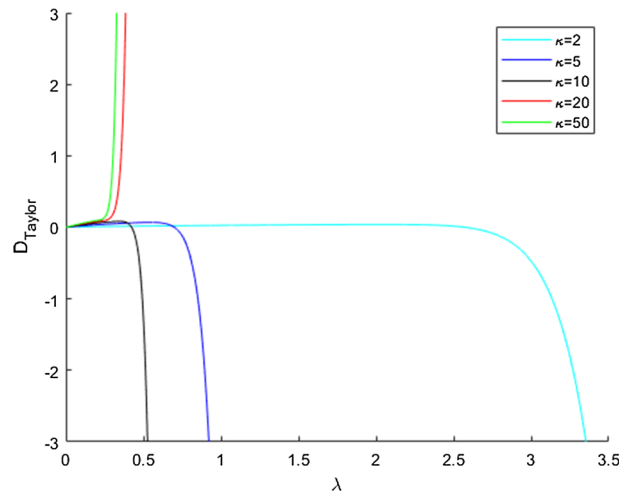


FIG. 3. Taylor deformation parameter ( $D_{Taylor}$ ) droplet as function of  $Ca_E$ , for different permittivity ratios  $\kappa$

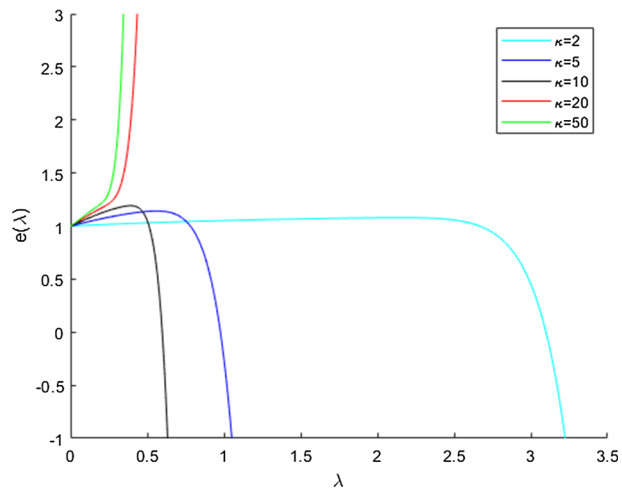


FIG. 4. The aspect ratio as function of  $Ca_E$ , for different permittivity ratios  $\kappa$

ratio  $e(\lambda)$  versus the electric capillary number  $\lambda$  in Fig. 4. This finding is consistent with the assertions of Miksis [22].

It is important to note that under a weak electric field, the drop deformation will also be small as illustrated in Fig. 5. We also illustrate in this figure a comparison between the analytical result, i.e. Eq.37 and those obtained by O’Konski and Thacher/Allan and Mason (OTAM). In the neighbourhood of  $\kappa = 1$ , the results are substantially the same, elsewhere the results differ due to the contribution of the second order in the formula Eq.37.

In Figs. 6 and 7, we plot the cross-section of the drop for various values of the electric capillary number, using a 15-term series for  $f(\theta, \lambda)$ . We observe that the deformation of the drop is smooth and the shape remains spherical.

For a fixed  $\kappa < 18$ , the drop flattens as  $\lambda$  progressively increases from values greater than  $\lambda_c$ , as illustrated in Fig. 6, which theoretically corresponds to unstable equilibrium family of axisymmetric drops.

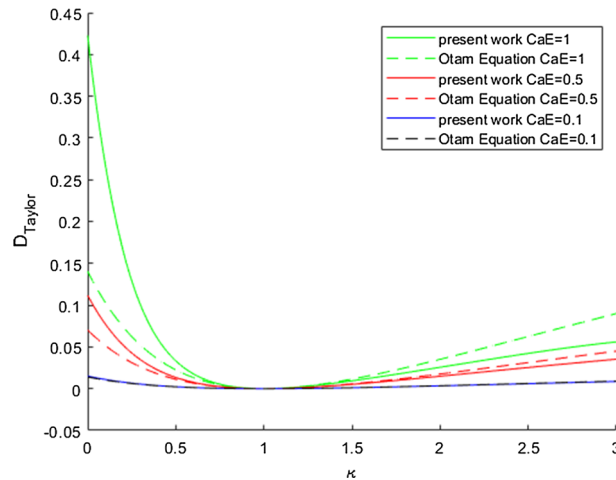


FIG. 5. Comparison between the present analytical results, and the OTAM equation. The diagram is drawn based on the deformation parameter  $D_{Taylor}$  versus the dielectric ratio for three electric capillary numbers

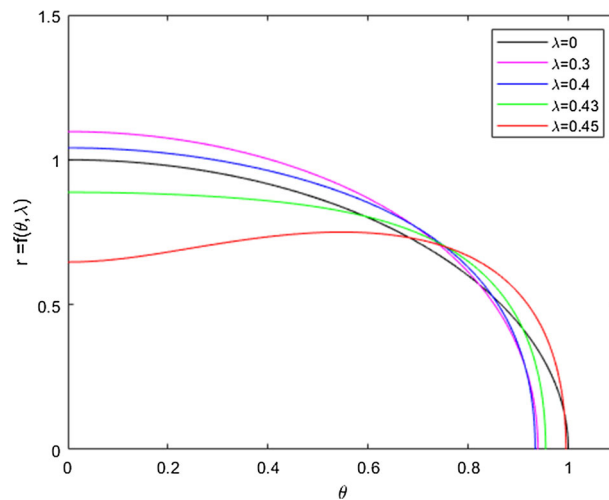


FIG. 6. Equilibrium shape for different values of  $Ca_E, \kappa = 10$

For a larger value of  $\kappa$ , the drop shape changes continuously from spherical figure to an elongated one when  $Ca_E$  varies, as shown in Fig. 7.

Below 3D deformed configurations of a drop immersed in a uniform electric field are illustrated in Figs. 8 and 9. The previous observations are confirmed. It appears that these figures elucidate that the increase of the electric field results in a drop elongation in the direction of the applied electric field. In Fig. 8, we can see the shape of the drop when  $\lambda$  reaches the critical value  $\lambda_c = 0.1946$  for the associated value of  $\kappa$ . Likewise Fig. 9 corresponds to  $\lambda_c = 0.2347$  and  $\kappa = 20$ .

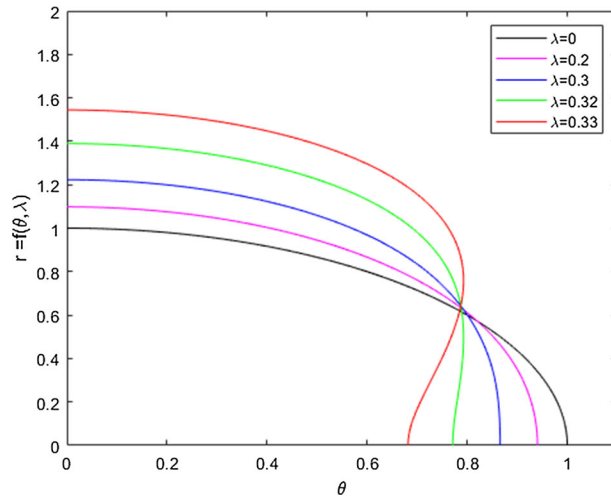


FIG. 7. Equilibrium shape for different values of  $Ca_E, \kappa = 50$

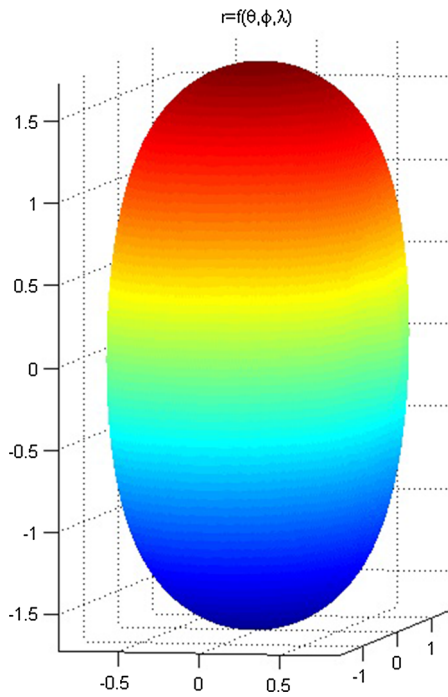


FIG. 8. The deformation of a dielectric drop in an electrical medium subjected to a uniform electric field under the values  $\lambda_c = 0.1946$  and  $\kappa = 50$

### 7. Conclusion

This work focused on the deformation study of a perfect dielectric drop subject to an electric field, magnetic and gravity effects being neglected. An analytical approach based on the perturbation domain

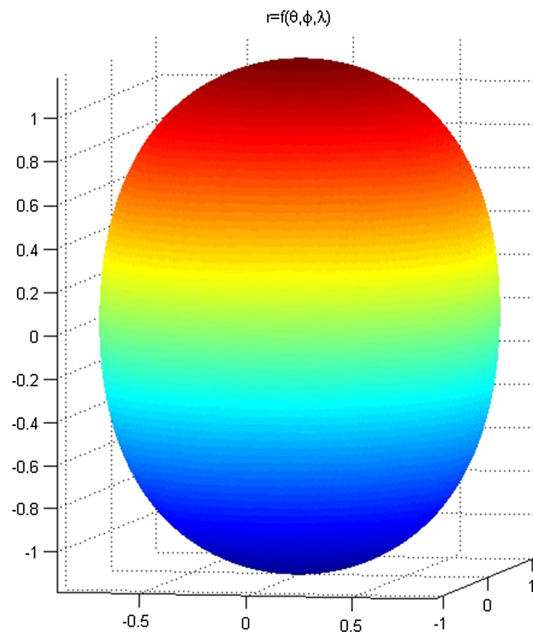


FIG. 9. The deformation of an electric drop in an electrical medium subjected to a uniform electric field under the values  $\lambda_c = 0.2347$  and  $\kappa = 20$

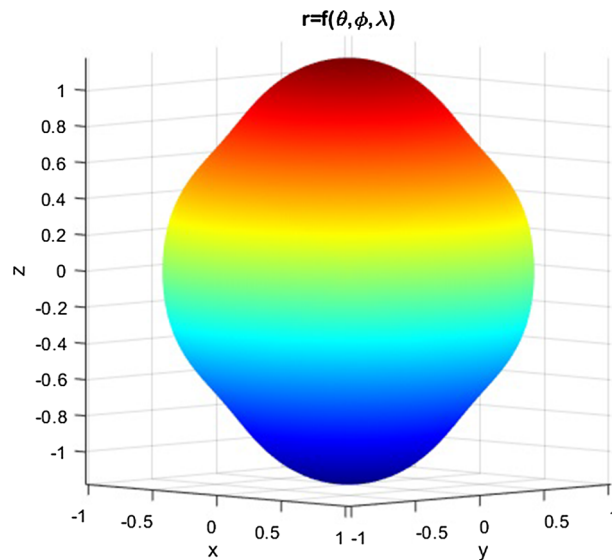


FIG. 10. A drop with conical ends under the values  $\lambda = 0.45$  and  $\kappa = 20$

method has been developed to derive the equilibrium drop shapes. This approach associated with the use of a special type of Hermite–Padé approximation, has made it possible to determine a critical value of the electric capillary number  $Ca_E$  depending on the ratio of the permittivities, leading to a subcritical



bifurcation, in the sense that beyond this critical value, the drop breaks, giving rise to several unstable droplets.

Even if this analytical approach allowed us to study the deformation of drops subjected to an electric field, it failed to reveal the existence of a family of conical shapes as Taylor stated in his paper [17] and confirmed by other authors like ([22, 24, 26, 28]).

These last authors even estimated a critical value of  $\kappa$  which are appreciably close to 17.59, for an external electric field being of order  $\frac{1}{\sqrt{F}}$  giving rise to drop shapes with conical tips. However, we can draw unstable figures resembling to conical shapes for a permittivity ratio  $\kappa > 18$  as it is illustrated in Fig. 10.

**Publisher's Note** Springer Nature remains neutral with regard to jurisdictional claims in published maps and institutional affiliations.

## References

- [1] Yangsoo, S., Kim, C.: Spreading of inkjet droplet of non-Newtonian fluid on solid surface with controlled contact angle at low Weber and Reynolds numbers. *J. Non-Newtonian Fluid Mech.* **162**(1–3), 78–87 (2009)
- [2] Bailey, G.: *Electrostatic Spraying of Liquids*. Wiley, New York (1988)
- [3] Bienia, M., Quilliet, C., Vallade, M.: Modification of drop shape controlled by electrowetting. *Langmuir* **19**(22), 9328–9333 (2003)
- [4] Keparle, P.: A brief overview of the present status of the mechanisms involved in electrospray mass spectrometry. *J. Mass Spectrom.* **35**, 804–817 (2000)
- [5] Brandenbourger, M., Caps, H., Vitry, Y., Dorbolo, S.: Electrically charged droplets in microgravity. *Microgravity Sci. Technol.* **29**(3), 229–239 (2017)
- [6] Song, H., Chen, D.L., Ismagilov, R.F.: Reactions in droplets in microfluidic channels. *Angewandte Chemie International Edition* **45**, 7336–7356 (2006)
- [7] Zaghdoudi, M.C., Lallemand, M.: Electric field effects on pool boiling. *J. Enhanced Heat Transf.* **9**(5–6), 187–208 (2002)
- [8] McDonald, J.E.: The shape and aerodynamics of large raindrops. *J. Meteorol.* **11**(6), 478–494 (1954)
- [9] Beard, K.V., Feng, J., Chuang, C.C.: A Simple perturbation model for the electrostatic shape of falling drops. *J. Atmos. Sci.* **46**(15), 2404–2418 (1989)
- [10] Thiam, A.R., Bremond, N., Bibette, J.: Breaking of an emulsion under an ac electric field. *Phys. Rev. Lett.* **102**, 188304 (2009)
- [11] Drelich, J., Bryll, G., Kapczynski, J., Hupka, J., Miller, J.D., Hanson, F.V.: The effect of electric field pulsation frequency on breaking water-in-oil emulsions. *Fuel Process. Technol.* **31**(2), 105–113 (1992)
- [12] Bernard Cohen, I.: *Benjamin Franklin's Experiments: A New Edition of Franklin's Experiments and observations on electricity*. Harvard University Press, Cambridge (1941)
- [13] Rayleigh, Lord: On the equilibrium of liquid conducting masses charged with electricity. *Philos. Mag.* **14**, 184–186 (1882)
- [14] O'Konski, C.T., Thacher, H.C.: The distortion of aerosol droplets by an electric field. *J. Phys. Chem.* **57**, 955–958 (1953)
- [15] Allan, R.S., Mason, S.G.: Particle behaviour in shear and electric fields I. Deformation and burst of fluid drops. *Proc. R. Soc. Lond. A* **267**, 45–61 (1962)
- [16] Garton, C.G., Krasucki, Z.: Bubbles in insulating liquids: stability in an electric field. *Proc. R. Soc. Lond. A* **280**, 211–226 (1964)
- [17] Taylor, G.I.: Studies in electrohydrodynamics: I. The circulation produced in a drop by an electric field. *Proc. R. Soc. Lond. A* **280**, 383–397 (1966)
- [18] Taylor, G.I.: Disintegration of water drops in an electric field. *Proc. R. Soc. Lond. A* **291**, 159–166 (1964)
- [19] Saville, D.A.: Electrohydrodynamics: the Taylor–Melcher leaky dielectric model. *Annu. Rev. Fluid Mech.* **29**, 27–64 (1997)
- [20] Rosenkilde, C.E.: A dielectric fluid drop in an electric field. *Proc. R. Soc. Lond. A* **312**, 473–494 (1969)
- [21] Ajayi, O.O.: A note on Taylor's electrohydrodynamic theory. *Proc. Roy. Soc. Lond. A* **364**, 499–507 (1978)
- [22] Miksis, M.J.: Shape of a drop in an electric field. *Phys. Fluids* **24**, 1967–1972 (1981)
- [23] Dodgson, V., Sozou, C.: The deformation of a liquid drop by an electric field. *ZAMP* **38**, 424–432 (1987)
- [24] Sherwood, J.D.: Breakup of fluid droplets in electric and magnetic fields. *J. Fluid Mech.* **188**, 133–146 (1988)
- [25] Basaran, O.A., Scriven, L.E.: Axisymmetric shapes and stability of charged drops in an external electric field. *Phys. Fluids A* **1**, 799–809 (1989)
- [26] Li, H., Halsey, T.C., Lobkovsky, A.: Singular shape of a fluid drop in an electric or magnetic field. *Europhys. Lett.* **27**, 575–580 (1994)

- [27] Feng, J.Q., Scott, T.C.: A computational analysis of electrohydrodynamics of a leaky dielectric drop in an electric field. *J. Fluid Mech.* **311**, 289–326 (1996)
- [28] Stone, H.A., Lister, J.R., Brenner, M.P.: Drops with conical ends in electric and magnetic fields. *Proc. Roy. Soc. Lond. A* **455**, 329–347 (1999)
- [29] Shaw, S.J., Shaw, S.P.D.M.: Critical strength of an electric field whereby a bubble can adopt a steady shape. *Proc. R. Soc. A Math. Phys. Eng. Sci.* **465**(2110), 3127–3143 (2009)
- [30] Bjorklund, E.: The level-set method applied to droplet dynamics in the presence of an electric field. *Comput. Fluids* **38**(2), 358–369 (2009)
- [31] Paknemat, H., Pishevar, A.R., Pournaderi, P.: Numerical simulation of drop deformations and breakup modes caused by direct current electric fields. *Phys. Fluids* **24**, 102101 (2012)
- [32] Melcher, J.R., Taylor, G.I.: Electrohydrodynamics: a review of the role of interfacial shear stresses. *Annu. Rev. Fluid Mech.* **1**, 111–146 (1969)
- [33] Joseph, D.D.: Domain perturbations: the higher order theory of infinitesimal water waves. *Arch. Ration. Mech. Anal.* **51**, 295–303 (1973)
- [34] Sattinger D.H.: Topics in stability and bifurcation theory. Springer, Lecture Notes in Mathematics, 309 (1973)
- [35] Guttman, A.J.: Asymptotic analysis of power-series expansions. in *Phase Transitions and Critical Phenomena Vol. 13*, 1-234, eds C. Domb and J.L Lebowitz (Academic Press, New York) (1989)
- [36] Common, A.K.: Applications of Hermite–Padé approximants to water waves and the harmonic oscillator on a lattice. *J. Phys. A* **15**, 3665–3677 (1982)
- [37] Makinde, O.: On thermal stability of a reactive third-grade fluid in a channel with convective cooling the walls. *Appl. Math. Comput.* **213**(1), 170–176 (2009)
- [38] Er-Riani, M., El Jarroudi, M., Sero-Guillaume, O.: Hermite–Padé approximation approach to shapes of rotating drops. *Appl. Math. Mod.* **38**, 212–220 (2014)

Youness Filali, Mustapha Er-Riani and Mustapha El Jarroudi  
Department of Mathematics  
LMA, Faculty of Sciences and Techniques  
BP41690000 Tangier  
Morocco  
e-mail: filaliyouness29@gmail.com

Mustapha Er-Riani  
e-mail: merriani@uae.ac.ma

Mustapha El Jarroudi  
e-mail: eljarroudi@hotmail.com

(Received: April 16, 2020; revised: November 19, 2020; accepted: November 23, 2020)